Research Square

Preprints are preliminary reports that have not undergone peer review.
They should not be considered conclusive, used to inform clinical practice,
or referenced by the media as validated information.

Effects of sintering protocol and aging on the optical properties of multilayer zirconia

Joseane Silva
Universidade Federal de Santa Catarina
Ana Elisa Colle Kauling
Ludwig-Maximilians-Universität München
Mutlu Özcan
University of Zurich
Gustavo Nicolodelli
Universidade Federal de Santa Catarina
Claudia Angela Maziero Volpato
claudia.m.volpato@outlook.com

Universidade Federal de Santa Catarina

Research Article

Keywords: zirconia, color, translucency, fluorescence, sintering protocols

Posted Date: September 8th, 2026

DOI: https://doi.org/10.21203/rs.3.rs-10730971/v1

License: This work is licensed under a Creative Commons Attribution 4.0 International License.
Read Full License

Additional Declarations: No competing interests reported.

Effects of sintering protocol and aging on the optical properties of multilayer zirconia

Joseane Silva, DDS, MS, PhD,[a] Ana Elisa Colle Kauling, DDS, MS, PhD,[b] Mutlu Özcan, DDS, PhD,[c] Gustavo Nicolodelli, DDS, MS, PhD,[d] and Claudia Angela Maziero Volpato, DDS, MS, PhD[e]

[a] Researcher, Department of Dentistry, Health Sciences Center, Federal University of Santa Catarina, Florianópolis, Santa Catarina, Brazil.

[b] Researcher, Department of Prosthetic Dentistry, University Hospital, Ludwig-Maximilians-University, Munich, Germany.

[c] University of Zurich, Clinic for Masticatory Disorders and Dental Biomaterials, Center for Dental Medicine, Zurich, Switzerland.

[d] Adjunct Professor, Department of Physics, Center for Physical and Mathematical Sciences, Federal University of Santa Catarina, Florianópolis, Santa Catarina, Brazil.

[e] Full Professor, Department of Dentistry, Health Sciences Center, Federal University of Santa Catarina, Florianópolis, Santa Catarina, Brazil.

Corresponding author: Claudia Angela Maziero Volpato

ORCID: 0000-0003-0918-3678

Department of Dentistry - Health Sciences Center

Federal University of Santa Catarina (UFSC)

Trindade, Florianópolis, Santa Catarina, Brazil 88040-900

Email: claudia.m.volpato@ufsc.br / claudia.m.volpato@outlook.com

Effects of sintering protocol and aging on the optical properties of multilayer zirconia

ABSTRACT

Monolithic zirconia prostheses have been sintered using speed protocols; however, data regarding their optical properties and aging behavior remain scarce. This study evaluated the color, translucency, and fluorescence of multilayer translucent zirconias subjected to different sintering protocols and aging. A total of 120 0.8-mm-thick disks were made from Lava Esthetic Fluorescent Full-Contour Zirconia (LE group), IPS e.max ZirCAD Prime Esthetic (ZC group), and IPS e.max CAD (LD group). The zirconia specimens were obtained from the incisal (I), transitional (T), and body/dentin (B/D) zones. Half of the specimens were sintered using a standard protocol, while the other half underwent speed sintering. All specimens were aged in an autoclave. The L*a*b* coordinates and 3D excitation-emission matrices (EEMs) were obtained. ΔE_{00}, $\Delta L'$, $\Delta C'$, $\Delta H'$, TP_{00}, and ΔTP_{00} were calculated using CIEDE2000. Data were analyzed using Wilcoxon signed-rank, Mann-Whitney, and Kruskal-Wallis tests with Bonferroni correction (α=0.05). EEM contour plots were evaluated by Parallel Factor Analysis (CP/PARAFAC). The LEB group showed the highest ΔE_{00} (4.47) after speed sintering. Aging increased color differences under both sintering protocols, accompanied by a reduction in lightness (p<0.001). Translucency increased after speed sintering, except for ZCI. Reduced translucency was observed in ZCT, ZCD, and LD specimens after aging (p<0.001). Speed sintering and aging reduced fluorescence, with a more pronounced effect in the LE group. Speed sintering protocols can alter the color, translucency, and fluorescence of multilayer zirconia over time when combined with aging.

Keywords: zirconia; color; translucency; fluorescence; sintering protocols.

INTRODUCTION

Multi-layered zirconia was developed for monolithic crowns to overcome the esthetic limitations of 3 mol% yttria-stabilized tetragonal zirconia polycrystal (3Y-TZP) [1]. These zirconia blocks feature cervical, transitional, and incisal gradient zones to reproduce the shade of the dental structure [2,3]. The improved translucency of these materials is attributed to their higher yttria content (5% to 8%), the presence of mixed tetragonal and cubic phases, and a reduction in grain size (below 100 nm) [4].

Monolithic zirconia prostheses are typically milled from blocks in the green compact state and then sintered at high temperatures (approximately 1350 °C to 1550 °C) [5,6]. Studies have proposed modifications to standard sintering protocols by increasing the temperature and decreasing the overall sintering time [7,8]. These speed and super-speed sintering protocols involve speed heating, a short holding period at the peak temperature, and accelerated cooling [5]. The total cycle duration for these protocols ranges from 10 to 240 minutes, whereas standard sintering generally requires 5 to 12 hours, depending on the material's composition and microstructure [5,6].

Speed sintering protocols aim to optimize laboratory workflow by increasing productivity and reducing labor time and energy consumption [7,8]. These protocols can be made in portable furnaces, allowing prostheses to be fabricated during the patient's appointment and thereby reducing the number of clinical visits [7,9]. In addition, these methods can produce dense Y-TZP with ultrafine grain sizes [10-12], which enhance translucency [13]. Nonetheless, variations in parameters such as heating rate, holding time, and peak temperature can influence the optical and mechanical properties of zirconia by modifying its crystalline phases and final microstructure [7,11,14].

During sintering, grain growth increases with rising temperature [15], reducing intergranular pores and resulting in higher final zirconia density and a decrease in light scattering [8,16]. Studies have evaluated zirconia translucency after standard and speed sintering protocols [7,9,17-21], comparing it with lithium disilicate glass ceramics [17,22], including assessments after accelerated aging [8,22]. A systematic review reported that speed sintering generally does not significantly affect the translucency parameter (TP_{00}) [5]; however, other studies have observed reduced translucency [9,17,20,21,23], particularly in 5Y-PSZ [21]. Reduced translucency was also observed across the enamel, transitional, and dentin zones of multi-layered zirconia [9,24].

Color stability was evaluated after speed and ultra-speed sintering protocols, with sintering times ranging from 10 minutes to 2 hours [9,18,20,21,25,26]. Color differences of 0.5 to 1.2ΔE_{ab} were reported for 3Y-TZP and 5Y-TZP after these protocols [18]. Values of 2.98 (cervical zone), 2.19 (transition zone), and 2.22ΔE_{00} (incisal zone) were observed in multilayer zirconia [25,26], while differences ranging from 3.33 to 13.15ΔE_{00} were associated with varying dipping times [20]. The changes observed may be related to the concentrations of pigments present in the different zones [27,28]. However, zirconia aging was not evaluated in these studies.

Pure zirconia does not exhibit intrinsic fluorescence because it is a polycrystalline material without a glassy matrix [29], requiring industrial strategies such as doping with rare-earth elements (e.g., thulium [Tm_2O_3]-doped zirconia) [30] or the use of fluorescent glazing agents [31]. The fluorescence of 5Y-PSZ and 3Y-TZP zirconias has been evaluated after standard sintering, in comparison with bovine enamel, bovine dentin, and lithium disilicate [32]. Speed sintering protocols have not been assessed. Bovine dentin exhibited the highest fluorescence (peak at 430 nm), followed by enamel and the 5Y-PSZ zirconia material (Lava Esthetic, 3M ESPE). Although

studies have investigated the optical behavior of multi-layered zirconia after speed sintering, information regarding fluorescence and aging remains limited. Therefore, this study evaluated color, translucency, and fluorescence of multi-layered zirconia compared with lithium disilicate after speed sintering and an accelerated aging protocol. The null hypotheses tested were that these optical properties remain stable following the sintering and aging protocols.

MATERIAL AND METHODS

Two multi-layered translucent zirconia blocks (Lava Esthetic Fluorescent Full-Contour Zirconia; Solventum and IPS e.max ZirCAD Prime Esthetic; Ivoclar Vivadent), A2 shade, were milled (PrograMill; Ivoclar Vivadent) into Ø12-mm cylinders (n=16). The incisal, transition, and body/dentin zones were identified in each cylinder according to the translucency differences indicated by the manufacturers. The marked cylinders were sectioned using a low-speed steel disk (Duraflex; American Burrs). The resulting Ø12×1.0-mm disks for each layer (n=16 per zone) were polished on both sides (#800 and #1200; 3M), and the thickness was controlled with a digital micrometer (0.25/0.01 mm; Mitutoyo).

Lithium disilicate blocks (MT, A2 shade, IPS e.max CAD; Ivoclar Vivadent) were sectioned using a precision cutting machine (Isomet 1000; Buehler) to obtain comparative specimens. These specimens (n=16) were finished with aluminum oxide abrasive papers (#800 and #1200 grit) and the thickness was verified using a digital micrometer (0.25/0.01 mm; Mitutoyo). Sample size (n=8 per condition) was previously calculated, with a power of 80% and a type I error of 5%. The materials, groups, and subgroups are presented in Table 1.

Half of the specimens (n=8 per material) were subjected to the standard sintering protocol according to the manufacturer's instructions, while the other half was speed-sintered (Programat

P310; Ivoclar Vivadent). The sintering protocols and times are presented in Table 2. After sintering, the zirconia disks measured Ø10×0.8-mm dimensions. To simulate clinical conditions, two layers of glaze were applied with a brush to the disks, which were then fired in a furnace (Programat P310; Ivoclar Vivadent). Glaze powder (Ivocolor; Ivoclar Vivadent) was used for the LE group, whereas glaze powder containing incorporated fluorescent agents (Ivocolor Fluo; Ivoclar Vivadent) was applied to the ZC and LD groups.

All specimens were aged in an autoclave (Vitale Class 12; Cristófoli Biossegurança) at 134 ±2 °C under a 0.2-MPa pressure for 5 hours. According to Chevalier et al. [33], 1 hour of autoclave aging at 134 °C is equivalent to 3 to 4 years of in vivo zirconia aging.

To evaluate color and translucency, all specimens were measured on a spectrophotometer (Minolta CM-3600d; Konica Minolta) before (T_0) and after aging (T_1). Clean and dry specimens were positioned on white (standard calibration tile, L*: 93.7, a*: -1.5, b*: 3.9) and black (standard calibration tile, L*: 6.7, a*: -0.1, b*: 1.4) backgrounds and measured three times at their center by the same operator (C.A.M.V.). Propylene glycol (Labsynth Products Laboratories) was applied between the bottom surface of the specimens and the background tiles [34]. Measurements were made in reflectance mode with the following setup: d/8-degree, 2-degree standard observer, 360 to 740 nm wavelength (10 nm interval), 3-mm small area view (SAV), specular component excluded (SCE), UV component included, and CIE standard D65 illuminant. The validity and repeatability of the spectrophotometer were specified in the manufacturer's instructions (white calibration plate measured 30 times at 10 seconds, spectral reflectance: ±0.1%, and colorimetric values: ±0.02 ΔE_{ab}).

One specimen from each condition/time was prepared together with additional unglazed specimens to assess fluorescence. Three-dimensional (3D) fluorescence spectroscopy

measurements of excitation-emission matrices (EEM) were performed using a fluorescence spectrophotometer (F-7000, Hitachi), always by the same operator (G.N). The fluorescence EEM signal was obtained over the 240-550 nm range when excited between 280 and 600 nm. The excitation and emission slit widths were set to either 5 nm, and excitation and emission sampling intervals were 10.0 nm, with a scan speed of 2400 nm/min.

Color (ΔE_{00}), lightness ($\Delta L'$), chroma ($\Delta C'$), and hue ($\Delta H'$) differences were calculated using the CIEDE2000 formula [35,36]:

$$\Delta E_{00} = \left[\left(\frac{\Delta L'}{K_L S_L}\right)^2 + \left(\frac{\Delta C'}{K_C S_C}\right)^2 + \left(\frac{\Delta H'}{K_H S_H}\right)^2 + R_T\left(\frac{\Delta C'}{K_C S_C}\right)\left(\frac{\Delta H'}{K_H S_H}\right)\right]^{1/2}, \text{where}$$

$\Delta L'$, $\Delta C'$, and $\Delta H'$ represent the differences in lightness, chroma, and hue, respectively; R_T is a rotation function describing the interaction between chroma and hue in the blue region; S_L, S_C, and S_H are weighting functions, and K_L, K_C, and K_H are parametric factors, which were set to 1 in the present study [35]. The mean L*a*b* coordinates after standard sintering (T_0) were used as the reference for calculating these references.

The following formula was used to calculate the translucency parameter (TP_{00}) [37]:

$$TP_{00} = \left[\left(\frac{L'_B - L'_w}{k_L S_L}\right)^2 + \left(\frac{C'_B - C'_w}{k_C S_C}\right)^2 + \left(\frac{H'_B - H'_w}{k_H S_H}\right)^2 + R_T\left(\frac{C'_B - C'_w}{k_C S_C}\right)\left(\frac{H'_B - H'_w}{k_H S_H}\right)\right]^{1/2}, \text{where}$$

L', C', and H' represent lightness, chroma, and hue measured against black (b) and white (w) backgrounds. R_T (rotation function) accounts for the interaction between $\Delta C'$ and $\Delta H'$ in the blue region. The weighting functions (S_L, S_C, and S_H) adjust the overall color difference according to the position of the difference pair in the L', a', and b' coordinates. The parametric factor values were set to $k_L=k_C=k_H=1$ in the present study [38]. Additionally, the differences in translucency parameters (ΔTP_{00}) were calculated following [39]:

$$\Delta TP_{00} = TP_{before} - TP_{after}$$

After acquiring the EEMs, their contour plots were analyzed individually. In addition, the EEM spectra could be used for qualitative and quantitative characterization of fluorophores when combined with advanced multivariate statistical techniques, such CP/PARAFAC, which can decompose the complex fluorescence spectral signal into a combination of simple components [40]. The choice of components was based on the analysis of the consistency of the central tensor (Core consistency diagnostics - CONCORDIA) [41].

The 50:50% perceptibility and acceptability thresholds were used to correlate the clinical relevance of the findings [37,42]. The Wilcoxon signed rank test was used to compare times (T_0 vs. T_1), and the Mann-Whitney test was used to compare treatments (standard vs. speed). The Kruskal-Wallis test was applied to compare groups and zones, with Bonferroni correction for multiple comparisons (α=0.05). Statistical significance was set at $p<0.05$. Data analysis was made using statistical software (IBM SPSS Statistics, version 26.0; IBM Corp.).

RESULTS

Non-parametric tests were used, since normality was not identified by Shapiro-Wilk ($p<0.05$). Table 3 presents the mean values for the ΔE_{00}, $\Delta L'$, $\Delta C'$, and $\Delta H'$ of the materials, sintering protocols, and times, in addition to the statistical behavior found by the non-parametric tests. Color differences (ΔE_{00}) found in the present study ranged from 0.35 (for LD) to 4.47 (for LEB) after speed sintering protocol ($p<0.001$). The LE group showed the greatest ΔE_{00} values after speed sintering across all evaluated zones (incisal, transitional, and body).

Aging significantly affected color under both sintering conditions, with an increase in ΔE_{00} ($p<0.001$). Although the LE group exhibited the greatest ΔE_{00} after speed sintering (particularly

the LEB), the ΔE_{00} observed before and after aging were more pronounced in the ZC group. The LD group showed color differences below 1 ΔE_{00} after aging (p<0.001). According to the color differences thresholds described in the literature [42], the highest values found for LEB can be classified as clearly unacceptable (>3.6–≤5.4 ΔE_{00}). Most ΔE_{00} values observed after speed sintering and aging were within the acceptable (>0.8–≤1.8) to moderately unacceptable (>1.8–≤3.6) ranges for both zirconias (Figure 1).

Speed sintering affected lightness, reducing it in LEB and LEI specimens, and increasing it in LD. Lightness remained stable in LET, ZCI, ZCT, and ZCD after speed sintering, but decreased in most groups after aging (P<.001). The saturation varied among the tested materials. LEI specimens tended toward red (+a*) and blue (−b*) after speed sintering and aging, whereas LET and LEB tended toward green (−a*) and blue (−b*). For ZRI, a trend toward red (+a*) and yellow (+b*) was observed after sintering protocols and aging. A shift toward blue (−b*) was found in ZRT and ZRD specimens after aging. Saturation of the LD group remained stable after standard sintering, while a slight shift toward red (+a*) and blue (−b*) occurred after speed sintering.

The translucency parameter (TP_{00}) values and the translucency parameters differences (ΔTP_{00}) are shown in Table 4. Translucency increased after speed sintering, except for ZCI (p<0.001). The same behavior was observed in the LE (I, T, and B) after aging under both sintering protocols. Reduced translucency was observed in ZCT, ZCD, and LD specimens after aging (T_1). The greatest ΔTP_{00} values were found in the LE group, in comparisons between sintering protocols and between times. The LEI exhibited the largest ΔTP_{00} (2.12) after speed sintering and aging. This difference is considered acceptable according to the perceptibility and acceptability thresholds (>0.62 to ≤2.62) reported in literature [37]. The smallest ΔTP_{00} values were found in

the ZC group, followed by the LD group, and were considered imperceptible values. P-values of the multiple comparison of the groups (Kruskal-Wallis test) corrected by Bonferroni's test are presented in Supplementary Material - Table 1.

EMMs for sintering protocols and times are shown in Figures 2 and 3. Scattering effects (Rayleigh and Raman scattering) can be observed diagonally in all EEMs [43]. This effect was treated and removed using MATLAB software by applying the Zeep method [44]. After decomposing the EEM data by CP/PARAFAC, two fluorophores were found: F1) exhibiting a well-defined peak at an excitation wavelength of 310 nm and an emission wavelength of 385 nm, and F2) characterized by a peak at 320 nm excitation and 445 nm emission.

The highest fluorescence emission resulted from F1 in ZCD. Most specimens showed a reduction in fluorescence after speed sintering and aging. The fluorescence emitted by F1 appears to be related to the glaze applied on the ZC and LD surfaces (Figure 4). In uncoated specimens, fluorescence decreased, often becoming undetectable for F1, while the fluorescence emitted by F2 was notably prominent in the LE specimens (with or without glazing).

DISCUSSION

This study investigated the influence of sintering protocols and aging on the optical properties of esthetic materials used in monolithic prostheses. The null hypotheses were rejected, since the ΔE_{00}, TP_{00} values, and fluorescence intensity demonstrated that both speed sintering and aging affected the optical properties of the evaluated materials.

Speed sintering affected the color of all specimens, with variations in lightness and saturation. Studies have also reported color differences, especially in saturation, due to the different oxides and their concentrations used in the zones of multilayer zirconia [9,25,26].

Translucency increase was also observed after speed sintering in all groups (except ZCI). In speed sintering, the rapid temperature increase and shorter dwell time can result in distinct sintering behaviors across zones with different yttria contents, influencing grain growth and causing variations in sintering density that may subsequently affect the optical properties of multilayered zirconia [26]. Conversely, longer sintering times can promote the precipitation of the cubic phase and consequently increase the cubic zirconia content, resulting in more translucent materials [21].

However, the optical behavior of multilayer zirconias is considerably more complex, as it depends on variations in yttrium oxide (Y_2O_3) content and the distribution of different pigments across the block, resulting in differences in shade and translucency [3,27]. The addition of iron oxide (Fe_2O_3) can reduce the translucency of these blocks [24], whereas the incorporation of cerium (Ce) and bismuth (Bi) can significantly increase the b* coordinate [28], as observed in the ZRI specimens of the present study.

Aging produced acceptable ΔE_{00} values for the LE and ZC groups under both sintering protocols. Although zirconia is known to undergo aging when exposed to a moist oral environment [33], translucent zirconia showed greater aging resistance due to its higher cubic phase content [8,22]. On the other hand, the LD samples showed minimal and acceptable color changes, with stable chroma and hue, confirming their resistance to thermal aging in both sintering protocols [45].

In the present study, fluorescence was assessed using EEM, a fast, selective, and sensitive technique whose main advantage is the ability to acquire complete information about the fluorescence characteristics by simultaneously varying the excitation and emission wavelengths [40]. The Rayleigh scattering effects observed in EEMs are a type of elastic scattering in which

photons from the excitation source bounce off molecules in solution and are scattered in multiple directions without energy loss.

Two fluorophores were detected using EEM-CP/PARAFAC, a potentially useful approach for evaluating complex samples by enabling the decomposition of fluorescent materials irrespective of EEM component complexity [40,43]. The F1 component, with excitation and emission maxima at 310 and 385 nm, respectively, was attributed to the intrinsic fluorescence of aromatic organic groups. The F2 component exhibited blue emission, which is consistent with zirconia-related luminescence contributions, such as defects or interfacial states. In addition, the emission profile of F2 is consistent with the presence of the glazing agent. Therefore, F2 is conservatively attributed to a combined contribution of zirconia-associated effects and potential glaze-related fluorophores [31]. These fluorophores, generally rare earth oxides, were incorporated into both the enamel powder (in ZC and LD) and the zirconia block (in LE).

To simulate clinical use, 0.8-mm-thick specimens were prepared, receiving two layers of glazing agent with or without an incorporated fluorescence component. Other studies also confirm the fluorescence emission by LE [32]. However, information about the fluorophore component responsible for these materials is not available from the manufacturers.

The results of the present study indicate that the optical properties of multilayer zirconia are influenced by both the chosen sintering protocol and aging. To prevent undesirable esthetic changes, sintering must strictly adhere to the manufacturer's recommendations. A limitation of this study is the lack of microstructural evaluation of the materials following speed sintering and aging. Future investigations should consider including other esthetic materials and assessing additional optical properties, such as opalescence.

CONCLUSIONS

Based on the findings of this in vitro study, the following conclusions were drawn:

- The speed sintering protocol produced the greatest color differences in the LEB, with a reduction in lightness after aging.
- Translucency increased following the speed sintering protocol in all groups except ZCI, whereas a decrease was observed in ZCT, ZCD, and LD after aging.
- The LD group exhibited the highest color and translucency stability after both speed sintering and aging.
- The degree of fluorescence decreased after speed sintering and aging, especially for the LE group.

CLINICAL IMPLICATIONS

Noticeable changes in color, translucency, and fluorescence may occur in monolithic prostheses made from multilayered zirconia blocks after speed sintering, especially over time.

STATEMENTS AND DECLARATIONS

- Funding: No funding was received from any public funding agencies or private donations for this research.
- Competing Interests: The authors declare that they have no financial or non-financial conflicts of interest, either directly or indirectly related to the work submitted for publication.
- Ethics Approval: This study did not require prior ethical approval.
- Informed Consent: As this was an in vitro study, informed consent was not required.
- Data Availability: All data supporting the results and analyses of this article are fully available within this submission, including supplementary material.
- Artificial Intelligence: No artificial intelligence tools were used in the writing, analysis, or interpretation of the data in this manuscript.

REFERENCES

1. Cesar PF, Miranda RBP, Santos KF, Scherrer S, Zhang Y. Recent advances in dental zirconia: 15 years of material and processing evolution. Dent Mater. 2024;40:824-36.

2. Kolakarnprasert N, Kaiser MR, Kim DK, Zhang Y. New multi-layered zirconias: Composition, microstructure and translucency. Dent Mater. 2019;35:797-806.

3. Vardhaman S, Borba M, Kaiser MR, Kim DK, Zhang Y. Optical and mechanical properties of the multi-transition zones of a translucent zirconia. J Esthet Restor Dent. 2025;37:525-32.

4. Pekkan G, Pekkan K, Bayindir BC, Özcan M, Karasu B. Factors affecting the translucency of monolithic zirconia ceramics: A review from materials science perspective. Dent Mater J. 2020;39:1-8.

5. Liu H, Inokoshi M, Xu K, Tonprasong W, Minakuchi S, Van Meerbeek B, et al. Does speed-sintering affect the optical and mechanical properties of yttria-stabilized zirconia? A systematic review and meta-analysis of *in-vitro* studies. Jpn Dent Sci Rev. 2023;59:312-28.

6. Jerman E, Wiedenmann F, Eichberger M, Reichert A, Stawarczyk B. Effect of high-speed sintering on the flexural strength of hydrothermal and thermo-mechanically aged zirconia materials. Dent Mater. 2020;36:1144-50.

7. Kaiser MR, Gierthmuehlen PC, Santos MB, Cava SS, Zhang Y. Speed sintering translucent zirconia for chairside one-visit dental restorations: Optical, mechanical, and wear characteristics. Ceram Int. 2017;43:10999-11005.

8. Cokic SM, Vleugels J, Van Meerbeek B, Camargo B, Willems E, Li M, et al. Mechanical properties, aging stability and translucency of speed-sintered zirconia for chairside restorations. Dent Mater. 2020;36:959-72.

9. Shohdy EIH, Sabet A, Sherif AH, Salah T. The effect of speed sintering on the optical properties and microstructure of multi-layered cubic zirconia. J Prosthodont. 2025;34:316-22.

10. Jiang L, Liao Y, Wan Q, Li W. Effects of sintering temperature and particle size on the translucency of zirconium dioxide dental ceramic. J Mater Sci Mater Med. 2011;22:2429-35.

11. Stawarczyk B, Özcan M, Hallmann L, Ender A, Mehl A, Hämmerlet CHF. The effect of zirconia sintering temperature on flexural strength, grain size, and contrast ratio. Clin Oral Investig. 2013;17:269-74.

12. Catramby MF, Vale AL, Santos HES, Elias CN. Effect of sintering process on microstructure, 4-point flexural strength, and grain size of yttria-stabilized tetragonal zirconia polycrystal for use in monolithic dental restorations. J Prosthet Dent. 2021;125:824.e1-824.e8.

13. Kim M-J, Ahn J-S, Kim J-H, Kim H-Y, Kim W-C. Effects of the sintering conditions of dental zirconia ceramics on the grain size and translucency. J Adv Prosthodont. 2013;5:161-6.

14. Denry I, Kelly JR. State of the art of zirconia for dental applications. Dent Mater. 2008;24:299-307.

15. Jansen JU, Lümkemann N, Letz I, Pfefferle R, Sener B, Stawarczyk B. Impact of high-speed sintering on translucency, phase content, grain sizes, and flexural strength of 3Y-TZP and 4Y-TZP zirconia materials. J Prosthet Dent. 2019;122:396-403.

16. Ebeid K, Wille S, Hamdy A, Salah T, El-Etreby A, Kern M. Effect of changes in sintering parameters on monolithic translucent zirconia. Dent Mater. 2014;30:e419-24.

17. Lawson NC, Maharishi A. Strength and translucency of zirconia after high-speed sintering. J Esthet Restor Dent. 2020;32:219-25.

18. Liu Y-C, Lin T-H, Lin Y-Y, Hu S-W, Liu J-F, Yang C-C, et al. Optical properties evaluation of rapid sintered translucent zirconia with two dental colorimeters. J Dent Sci. 2022,17:155-61.

19. Madruga CFL, Dal Piva AMO, Pereira GKR, Caneppele TMF, Valandro LF, Bottino MA. Sintering mode of a translucent Y-TZP: Effects on its biaxial flexure fatigue strength, surface morphology and translucency. J Esthet Restor Dent. 2022;34:1197-205.

20. Savas TY, Akin C. Effects of sintering protocol and dipping time on the optical properties of monolithic zirconia. J Prosthet Dent. 2022;127:801.e1-801.e8.

21. Salah K, Sherif AH, Mandour MH, Nossair SA. Optical effect of rapid sintering protocols on different types of zirconia. J Prosthet Dent. 2023;130:253.e1-253.e7.

22. Michailova M, Elsayed A, Fabel G, Edelhoff D, Zylla I-M, Stawarczyk B. Comparison between novel strength-gradient and color-gradient multilayered zirconia using conventional and high-speed sintering. J Mech Behav Biomed Mater. 2020;111:103977.

23. Kim H-K, Kim S-H. Comparison of the optical properties of pre-colored dental monolithic zirconia ceramics sintered in a conventional furnace versus a microwave oven. J Adv Prosthodont. 2017;9:394-401.

24. Alves M, Abreu L, Klippel G, Santos C, Strecker K. Mechanical properties and translucency of a multi-layered zirconia with color gradient for dental applications. Ceram Int. 2021;47:301-9.

25. Miura S, Shinka A, Koizumi H, Fujisawa M. Effect of speed sintering of monolithic zirconia with different yttria contents on color and crystal phase. Eur J Oral Sci. 2022;130:e12898.

26. Miura S, Tsukada S, Fujita T, Fujisawa M, Vallittu P, Lassila L. Effects of sintering protocols, yttria content, and zirconia thickness on the optical properties of monolithic zirconia. J Oral Sci. 2025;67:122-6.

27. Cokic SM, Li M, Huang S, Vleugels J, Van Meerbeek B, Zhang F. Coloring multilayer zirconia zirconia may affects its optical and mechanical properties. J Dent Res. 2024;103:1091-9.

28. Shah K, Holloway JA, Denry IL. Effect of coloring with various metal oxides on the microstructure, color, and flexural strength of 3Y-TZP. J Biomed Mater Res B Appl Biomater. 2008;87:329-37.

29. Shahmiri R, Standart OC, Hart JN, Sorrell CC. Optical properties of zirconia ceramics for esthetic dental restorations: A systematic review. J Prosthet Dent. 2018;119:36-46.

30. Nakamura T, Okamuta S, Nishida H, Usami H, Nakano Y, Wakabayashi K, et al. Fluorescence of thulium-doped translucent zirconia. Dent Mater J. 2018;37:1010-6.

31. Volpato CAM, Carvalho O, Volpato GM, Fredel MC, Silva FS, Pereira MR. Assessment of zirconia fluorescence after treatment with immersion in liquids, glass infiltration and aging. Ceram Int. 2021;47:27511-23.

32. Kim H-K. Optical and mechanical properties of highly translucent dental zirconia. Materials (Basel). 2020;13:3395.

33. Chevalier J, Cales B, Drouin JM. Low-temperature aging of Y-TZP ceramics. J Am Ceram Soc. 1999;82:2150-4.

34. Dozic A, Kleverlaan CJ, Meegdes M, van der Zel J, Feilzer AJ. The influence of porcelain layer thickness on the final shade of ceramic restorations. J Prosthet Dent. 2003;90:563-70.

35. Commission Internationale de l′Eclairage. Colorimetry. CIE Technical Report: CIE 015:2018. 4th ed; 2019.

36. Sharma G, Wencheng W, Dalal EN. The CIEDE2000 color-difference formula: Implementation notes, supplementary test data, and mathematical observations. Col Res Appl. 2005;30:21-30.

37. Salas M, Lucena C, Herrera LJ, Yebra A, Della Bona A, Pérez MM. Translucency thresholds for dental materials. Dent Mater. 2018;34:1168-74.

38. Bolt RA, Bosch JJ, Coops JC. Influence of window size in small-window color measurement, particularly of teeth. Phys Med Biol. 1994;39:1133-42.

39. Gasparik C, Culic B, Varvara MA, Grecu A, Burde A, Dudea D. Effect of accelerated staining and bleaching on chairside CAD/CAM materials with high and low translucency. Dent Mater J. 2019;38:987-93.

40. Bro R. PARAFAC. Tutorial and applications. Chemom Intell Lag Syst 1997;38:149-71.

41. Mounier S, Nicolodelli G, Redon R, Milori DMBP. Direct solid surface fluorescence spectroscopy of standard chemicals and humic acid in ternary system. Spectrochim Acta A Mol Biomol Spectrosc. 2017;177:79-85.

42. Paravina RD, Pérez MM, Ghinea R. Acceptability and perceptibility thresholds in dentistry: A comprehensive review of clinical and research applications. J Esthet Restor Dent. 2019;31:103-12.

43. Matos M, Tadino AM, Conceição FR, Machulek Junior A, Menegatti CR, Mounier S, et al. Dissolved organic matter in bovine slaughterhouse wastewater using fluorescence spectroscopy associated with CP/PARAFAC and PCA methods. Appl Optics. 2022;61:6590-8.

44. Zepp R, Moran MA. Dissolved organic fluorophores in southeastern US coastal waters: correction method for eliminating Rayleigh and Raman scattering peaks in excitation–emission matrices. Mar Chem. 2004;89:1-4.

45. Alasmari MA, Rayyan MR. Effect of aging on the translucency of lithium disilicate and zirconia reinforced lithium silicate ceramics: An *in vitro* study. Heliyon. 2024;10:e40757.

TABLES

Table 1. Groups and subgroups according to material and sintering protocols

Material	Description and composition	Group	Subgroup	Sintering protocol
Lava Esthetic Fluorescent Full Contour (batch 4514465)	5Y-PSZ ZrO_2, HfO_2, Y_2O_3, Al_2O_3, and other oxides	LE	Incisal zone: LEI Transition zone: LET Body zone: LEB	Standard Speed
IPS e.max ZirCAD, Prime Esthetic (batch Z04G4N)	4Y-TZP/5Y-TZP ZrO_2, HfO_2, Y_2O_3, Al_2O_3, and other oxides	ZC	Incisal zone: ZCI Transition zone: ZCT Dentin zone: ZCD	Standard Speed
IPS e.max CAD (batch YB552T)	Lithium disilicate glass ceramic SiO_2, Li_2O, K_2O, P_2O_5, ZrO_2, ZnO, Al_2O_3, MgO, and coloring oxides	LD	-	Standard Speed

Table 2. Standard and speed sintering protocols

Groups	Stage	Standard sintering protocol	Speed sintering protocol
LE	Heating	20 °C/min to 800 °C	60 °C/min to 1000 °C
		10 °C/min to 1500 °C	3 °C/min to 1530 °C
	Holding time	120 min at 1500 °C	60 min at 1530 °C
	Cooling	15 °C/min to 800 °C	50 °C/min to 1100 °C
		20 °C/min to 250 °C	60 °C/min to 100 °C
	Total time	303 min	205min
ZC	Heating	20 °C/min to 900 °C	60 °C/min to 1000 °C
		10 °C/min to 1500 °C	3 °C/min to 1530 °C
	Holding time	120 min at 1500 °C	60 min at 1530 °C
	Cooling	10 °C/min to 900 °C	50 °C/min to 1100 °C
		8 °C/min to 300 °C	60 °C/min to 100 °C
	Total time	440min	205min
LD	Closing time	Hold at 403 °C for 6 min	Hold at 403 °C for 30 s
	Holding time (T1)	60 °C/min to 780 °C (00:10)	120 °C/min to 850 °C (00:00)
	Holding time (T2)	30 °C/min to 860 °C (10:00)	70 °C/min to 870 °C (03:30)
	Vacum 1	550/780 °C	690/850 °C
	Vacum 2	780/860 °C	850/870 °C
	Cooling	Start at 710 °C	Start at 710 °C
	Total time	26 min	14.55 min

Table 3. Mean values of color (ΔE_{00}), lightness ($\Delta L'$), chroma ($\Delta C'$), and hue differences ($\Delta H'$) of groups and subgroups according to sintering protocols and aging times

			ΔE_{00}		$\Delta L'$		$\Delta C'$		$\Delta H'$	
Groups	Subgroups	Sintering Protocol	T_0	T_1	T_0	T_1	T_0	T_1	T_0	T_1
LE	LEI	Standard	0.24 ±0.15	0.42 ±0.18	0.00 ±0.18	-0.47 ±0.30§	0.01 ±0.40	-0.17 ±0.26	0.00 ±0.05	-0.06 ±0.10
		Speed	2.23 ±0.15*	2.60 ±0.20*§	-1.65 ±0.40*	-2.43 ±0.40*§	-2.63 ±0.49*	-2.69 ±0.44*	-0.33 ±0.15*	-0.34 ±0.07*
	LET	Standard	0.31 ±0.13	0.54 ±0.25	0.01 ±0.40	-0.30 ±0.10	0.00 ±0.29	-0.26 ±0.98	0.00 ±0.05	0.11 ±0.12§
		Speed	2.10 ±1.00*	3.36 ±0.67*§	-0.40 ±0.33*	-1.64 ±0.78*§	-3.38 ±1.75*	-4.96 ±1.69*	-0.54 ±0.13*	-0.54 ±0.38*
	LEB	Standard	0.35 ±0.11	0.44 ±0.08§	0.00 ±0.36	-0.21 ±0.38	0.01 ±0.38	-0.07 ±0.45	0.00 ±0.23	0.14 ±0.26
		Speed	4.47 ±0.96*	4.96 ±0.55*	-2.75 ±0.26*	-3.70 ±0.17*§	-3.82 ±1.66*	-4.21 ±0.86*	3.72 ±0.81*	3.83 ±0.45*
ZC	ZCI	Standard	0.40 ±0.16	2.22 ±0.17§	0.00 ±0.29	-2.79 ±0.23§	0.01 ±0.42	-0.51 ±0.19§	0.01 ±0.29	-0.70 ±0.24§
		Speed	0.50 ±0.19a	2.13 ±0.24§	-0.37 ±0.33	-2.49 ±0.31*§	0.23 ±0.13	-0.04 ±0.41*	-0.35 ±0.16*	-1.07 ±0.34*§
	ZCT	Standard	0.41 ±0.19	2.56 ±0.37§	0.00 ±0.48	-3.16 ±0.46§	0.01 ±0.46	-1.39 ±0.40§	0.00 ±0.16	-0.43 ±0.20§
		Speed	0.95 ±0.19*	3.23 ±0.54*§	0.35 ±0.23	-2.93 ±0.30§	1.45 ±1.87	-0.10 ±1.71§	3.00 ±0.70*	2.41 ±0.55*§
	ZCD	Standard	0.33 ±0.12	2.75 ±0.15§	0.00 ±0.36	-3.33 ±0.21§	0.01 ±0.38	-1.78 ±0.32§	0.00 ±0.17	-0.42 ±0.23§
		Speed	0.97 ±0.10*	2.30 ±0.32*§	0.49 ±0.20*	-2.84 ±0.48*§	1.31 ±0.31*	-0.68 ±0.36*§	-0.50 ±0.08*	-0.84 ±0.11*§
LD	-	Standard	0.23 ±0.13	0.35 ±0.14	0.00 ±0.28	-0.04 ±0.38	0.01 ±0.27	0.30 ±0.23	0.00 ±0.10	-0.08 ±0.16
		Speed	0.98 ±0.11*	0.96 ±0.11*	0.80 ±0.22*	0.45 ±0.45*	-1.10 ±0.38	-1.27 ±0.35*	-0.24 ±0.26*	-0.17 ±0.19
Comparison of all groups#		Standard	<0.001	<0.001	=0.999	<0.001	>0.999	<0.001	=0.961	=0.001
		Speed	<0.001	<0.001	<0.001	<0.001	<0.001	<0.001	<0.001	<0.001

LE: Lava Esthetic Fluorescent Full-Contour Zirconia Disc; ZC: IPS e.max ZirCAD Prime Esthetic; LEI: incisal zone; LET: transition zone; LEB: body zone; ZCI: incisal zone; ZCT: transition zone; LED: dentin zone; LD: IPS e.max CAD.

*: indicates a significant difference between the sintering protocols (standard vs speed sintering) ($p<0.05$).

§: indicates a significant difference between the times (T0 vc. T1) ($p<0.05$).

#: Comparison of the groups (LEI, LET, LEB, ZCI, ZCT, ZCD, LD) using Kruskal-Wallis test.

Table 4. Mean values of translucency parameters (TP_{00}) and translucency parameter differences (ΔTP_{00}) of the groups and subgroups according to different sintering protocols and aging times

Groups	Subgroups	Sintering Protocol	TP_{00} T_0	TP_{00} T_1	ΔTP_{00} T_0	ΔTP_{00} T_1
LE	LEI	Standard	6.40 ±0.20	7.97 ±0.28§	-	-1.57 ±0.36
		Speed	7.33 ±0.21*	9.45 ±0.32*§	-0.93 ±0.20	-2.12 ±0.32
	LET	Standard	6.85 ±0.02	8.85 ±0.52§	-	-2.00 ±0.52
		Speed	8.46 ±0.71*	8.63 ±0.75	-1.61 ±0.71	-0.17 ±0.89
	LEB	Standard	6.33 ±0.29	8.16 ±0.46§	-	-1.83 ±0.42
		Speed	7.88 ±0.26*	9.49 ±0.34*§	-1.55 ±0.21	-1.61 ±0.46
ZC	ZCI	Standard	8.94 ±0.34	9.22 ±0.29	-	-0.28 ±0.41
		Speed	8.86 ±0.24	9.47 ±0.32§	0.08 ±0.40	-0.61 ±0.40
	ZCT	Standard	6.43 ±0.34	6.45 ±0.35	-	-0.01 ±0.50
		Speed	7.55 ±0.78*	7.19 ±0.60*	-1.12 ±0.65	0.36 ±0.92
	ZCD	Standard	7.25 ±0.21	7.18 ±0.27	-	0.08 ±0.32
		Speed	7.35 ±0.19	6.82 ±0.30*§	-0.10 ±0.20	0.53 ±0.36
DL	-	Standard	9.63 ±0.26	9.76 ±0.20	-	-0.13 ±0.36
		Speed	10.14 ±0.23	9.70 ±0.25	-0.51 ±0.36	-0.43 ±0.34
Comparison of all groups$^{\#}$		Standard	<0.001	<0.001		
		Speed	<0.001	<0.001		

*: indicates a significant difference between the sintering protocols (standard vs speed sintering) (p<0.05).
§: indicates a significant difference between the times (T0 vc. T1) (p<0.05).
$^{\#}$: Comparison of the groups (LEI, LET, LEB, ZCI, ZCT, ZCD, LD) using Kruskal-Wallis test.

FIGURES

Fig 1 Color differences (ΔE_{00}) after speed sintering for groups and times

* 50:50% perceptibility and acceptability thresholds for acceptable matches on horizontal lines.

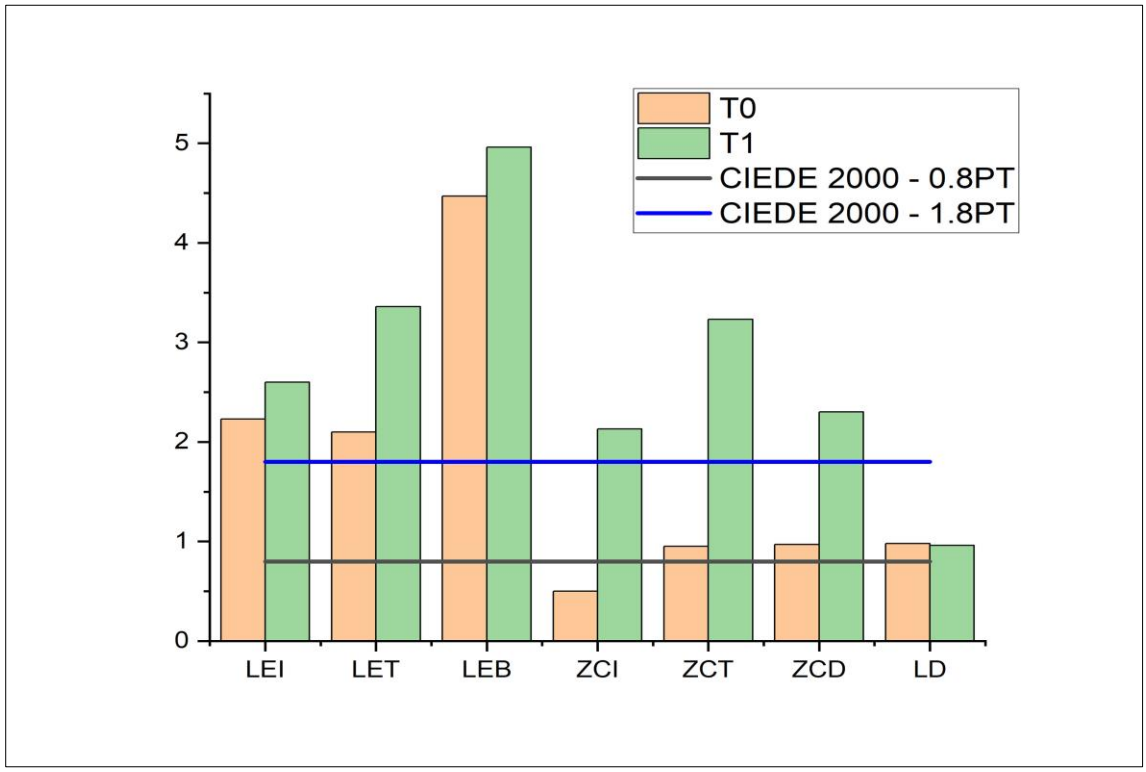
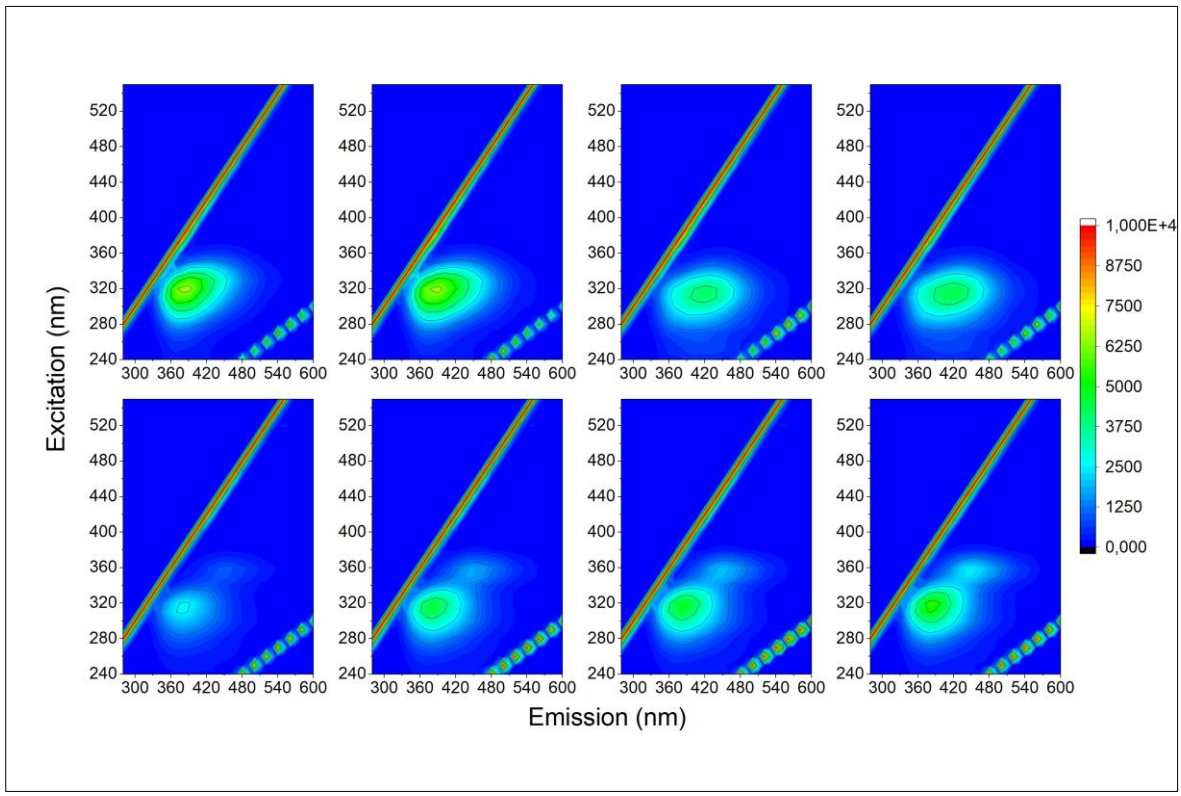
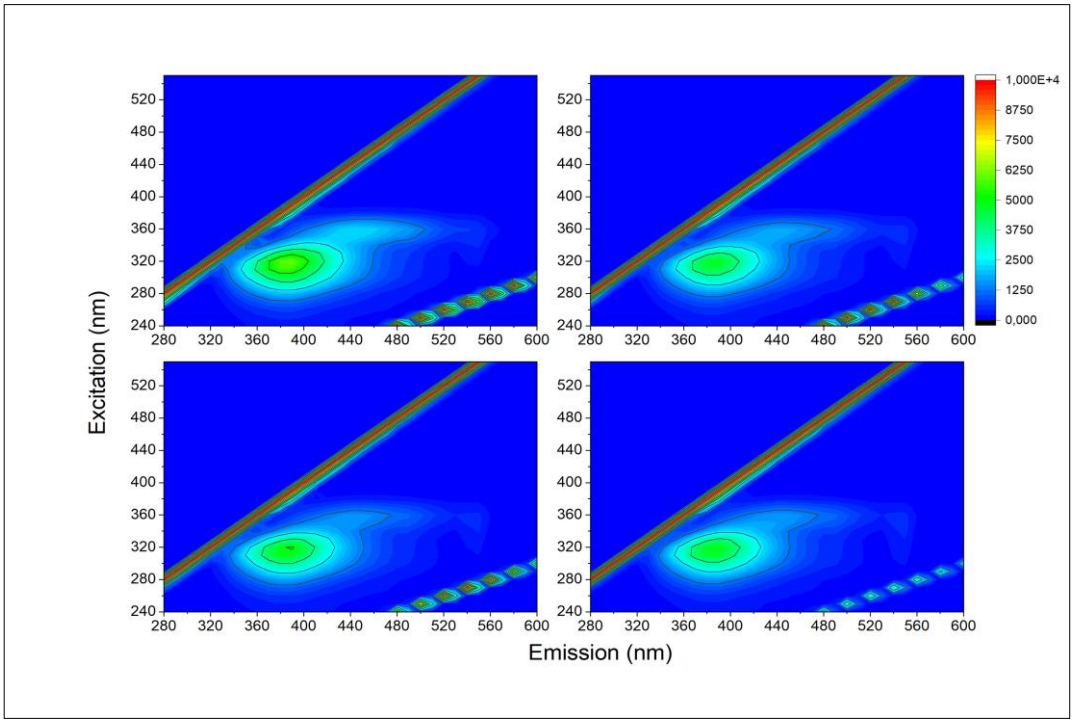


Fig 2 Representative 3D fluorescence maps of LEI and ZCI after standard and speed sintering without aging (T0) and after the aging protocol (T1)



*A, LEI/standard/T0. B, LEI/standard/T1. C, LEI/speed/T0. D, LEI/speed/T1. E, ZCI/standard/T0. F, ZCI/standard/T1. G, ZCI/speed/T0. H, ZCI/speed/T1.

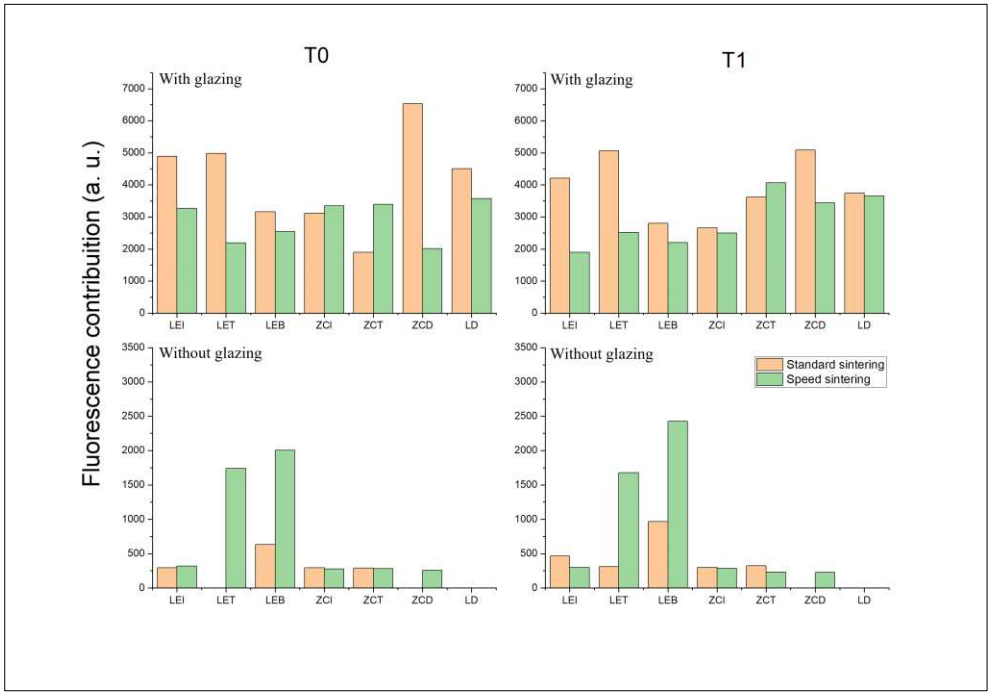
Fig 3 3D fluorescence maps of the LD group in standard and speed sintering protocols, before (T0) and after aging (T1)



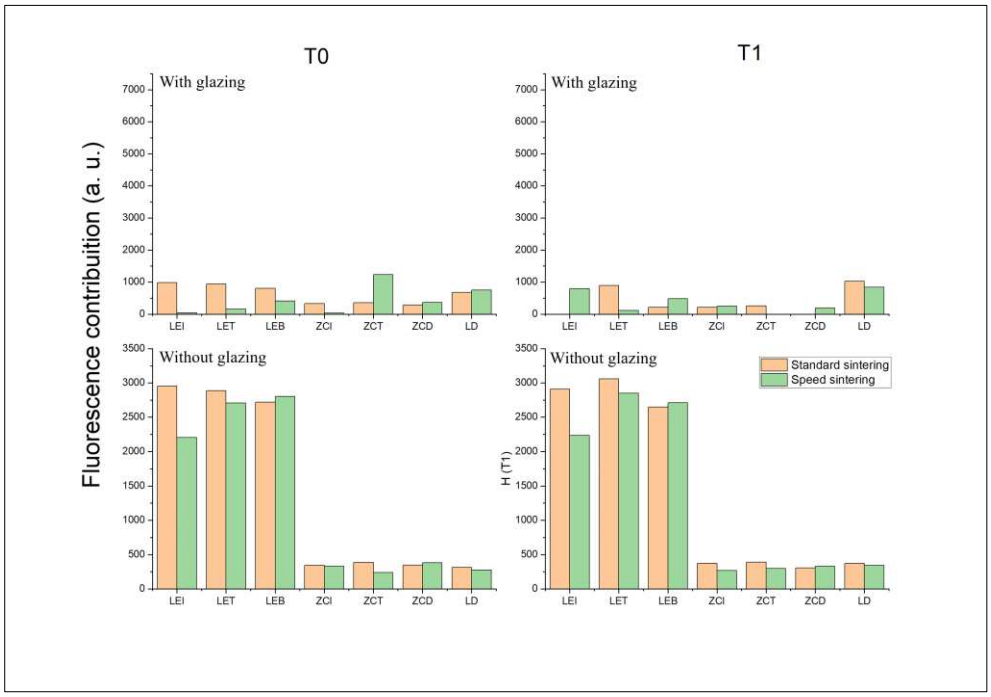
*A, LD/standard/T0. B, LD/speed/T0. C, LD/standard/T1. D, LD/speed/T1.

Fig 4 Fluorescence according to the contribution of the fluorophore agent found for the groups, sintering protocols, aging, and glazing. A, F1 and B, F2

A,



B,



a. u.= arbitraty units

Supplementary Files

This is a list of supplementary files associated with this preprint. Click to download.

- SupplementaryMaterialTable1.docx